JOURNAL OF COMPUTATIONAL PHYSICS 2, 277-302 (1967)

The Diffuse Reflection of Radiation by Model Planetary Atmospheres

I. P. GRANT

Pembroke College, Oxford, and the Atlas Computer Laboratory, Science Research Council, Chilton, Didcot, Berks., England

AND

V. M. BURKE

Atlas Computer Laboratory, Science Research Council, Chilton, Didcot, Berks., England

ABSTRACT

This paper describes a method for calculating line profiles and equivalent widths for the diffuse reflection of sunlight from a model planetary atmosphere. We base our numerical process on the method of invariant imbedding. The angular dependence of the diffuse reflection coefficient is approximated by a quadratic spline, which makes the calculation of reflected intensities particularly easy. We give an error analysis.

Finally, we describe the construction of a general program for performing the calculations, and some preliminary results obtained for a simple model of the Venus atmosphere are given to illustrate its potential.

I. INTRODUCTION

Recent work on the interpretation of the absorption bands of CO_2 in the near-infrared region of the spectrum of Venus suggests that they are produced by multiple scattering in an optically thick atmosphere [1], [2]. The nature of that atmosphere remains obscure.

Spinrad [3], has microphotometered the ten best old Mount Wilson 100-in coudé spectrograms of Venus, and has measured the equivalent widths of the 12 unblended *P*-branch lines in the λ-7820 CO_2 band at several different Venus phase angles. It is our aim to conduct numerical experiments in which we vary the parameters of simple models of the Venus atmosphere in an attempt to fit the observed line profiles and equivalent widths.

We suppose that the atmosphere is locally plane-parallel, so that all atmospheric properties can be regarded as a function of height above the surface of the planet.

We consider only monochromatic radiative transfer, and suppose that scattering of radiation is isotropic with a mean free path depending upon height. Absorption at each frequency within a spectral line depends upon the variation of temperature and pressure with height. We assume that thermal emission is negligible in the region of λ-7820.

We shall begin by discussing the analytic and numerical methods we use to solve the radiative transfer problem, and assessing their convenience and accuracy. Then we shall describe the specification of a simple atmospheric model, before passing to an outline of the construction of the SNARK computer code which generates the monochromatic diffuse reflection matrices which we need. We store these on magnetic tape, and use a separate code, the SNARK EDITOR, to generate from them the data to be compared with observation. Both codes have been constructed so as to reduce the amount of manual data handling to a minimum. Automatic graph-plotting devices are used to generate line profiles and other data, and so make it easy to compare models.

The paper closes with a description of the tests we have performed to justify our methods, and with an example of a production run. This is just one of a series of calculations on Venus which we hope to describe in detail elsewhere.

II. The Diffuse Reflection of Monochromatic Radiation from an Atmosphere

II.1 *The Diffuse Reflection Coefficient and its Use*

It is convenient to begin by defining the diffuse reflection coefficient. We consider some level in the atmosphere, and suppose it irradiated by a parallel beam of flux πF_ν per unit area. Let this beam make an angle $\pi - \theta_0$ with the outward directed vertical, and φ_0 with some fixed tangential direction. Then the specific intensity of radiation in the direction defined by angles θ and φ can be related to F_ν by the linear relation

$$I_\nu(\mu, \varphi) = \frac{F_\nu}{4\mu} S_\nu(\mu, \varphi; \mu_0, \varphi_0), \tag{2.1}$$

where $\mu = \cos\theta$, $\mu_0 = \cos\theta_0$, $0 \leq \theta$, $\theta_0 \leq \pi/2$, $0 \leq \varphi$, $\varphi_0 < 2\pi$. The coefficient S is the diffuse reflection coefficient. It satisfies an equation described in Section II.2.

We now suppose that the level at which we have computed S is sufficiently

high in the atmosphere so that reflection and attenuation from higher levels can be ignored. Equation (2.1) then describes the reflection from a localized area of the atmosphere. In Appendix A we show, that the specific intensity of radiation reflected in a fixed direction (making an angle $\cos^{-1}\bar{\mu}$ with the direction of the sun) can be written

$$I_\nu(\bar{\mu}) = \frac{F_\nu}{2\pi} \int_0^1 \int_{m(\mu,\bar{\mu})}^{M(\mu,\bar{\mu})} \frac{S_\nu(\mu, \varphi;\ \mu_0\ ,\ \varphi_0)\, d\mu_0\, d\mu}{[1 - \mu^2 - \mu_0{}^2 - \bar{\mu}^2 + 2\mu\mu_0\bar{\mu}]^{1/2}} \tag{2.2}$$

where

$$M(\mu, \bar{\mu}) = \mu\bar{\mu} + [(1 - \mu^2)\,(1 - \bar{\mu}^2)]^{1/2}\,,$$

$$m(\mu, \bar{\mu}) = \max\{0,\ \mu\bar{\mu} - [(1 - \mu^2)\,(1 - \bar{\mu}^2)]^{1/2}\},$$

$$\varphi = \pi,$$

$$\tan\varphi_0 = [1 - \mu^2 - \mu_0{}^2 - \bar{\mu}^2 + 2\mu\mu_0\bar{\mu}]^{1/2}/(\bar{\mu} - \mu\mu_0).$$

In the case of an isotropic scattering atmosphere, the S-coefficient becomes independent of φ and of φ_0. We restrict ourselves to this case in the future.

We can also compute the planetary albedo A_ν defined as the fraction of incident solar energy which is reradiated. Indeed

$$\pi F_\nu \cdot A_\nu = 2\pi \int_{-1}^{1} I_\nu(\bar{\mu})\, d\bar{\mu} \tag{2.3}$$

and we obtain easily

$$A_\nu = \int_0^1 \int_0^1 S_\nu(\mu, \mu_0)\, d\mu\, d\mu_0. \tag{2.4}$$

Likewise, we can calculate the albedo $a_\nu(\mu_0)$ of a localized area of the planet for radiation entering at an angle θ_0. From (2.1) the flux emerging from the atmosphere is

$$\pi H_\nu = \pi F_\nu \cdot \mu_0 \cdot a_\nu(\mu_0) = 2\pi \int_0^1 \mu I_\nu(\mu)\, d\mu$$

so that

$$a_\nu(\mu_0) = \frac{1}{2\mu_0} \int_0^1 S_\nu(\mu, \mu_0)\, d\mu \tag{2.5}$$

By using the fact that the amount of radiation entering the atmosphere with $\cos\theta_0$ in the range μ_0 to $\mu_0 + d\mu_0$ is $\pi F_\nu \cdot 2\mu_0\, d\mu_0$, we recover (2.4).

II.2 *Line Profiles and Equivalent Widths*

The specific intensity measured by a hypothetical detector on earth will be given by Eq. (2.1) or (2.2), or by some similar expression. Near an isolated absorption line, center ν_J, the specific intensity will be reduced. If we denote the specific intensity in the far wings of the line by $I_\infty(\mu, \varphi)$ [or $I_\infty(\mu)$], we can define the line profile as the ratio $I_\nu(\mu)/I_\infty(\mu)$ for all values of ν. It is in this sense that we shall use the term.

We can define the equivalent width by the relation

$$W(\mu, \varphi) = \int_{\Delta\nu} [1 - I_\nu(\mu, \varphi)/I_\infty(\mu, \varphi)]\, d\nu \tag{2.6}$$

where $\Delta\nu$ denotes the interval $(\nu_J - \Delta\nu_-, \nu_J + \Delta\nu_+)$, say $(\Delta\nu_-, \Delta\nu_+ > 0)$. The equivalent width is effectively the frequency spread of a completely black line giving the same total absorption. Provided the line is formed in a region of the spectrum far from any solar line, we may assume that the incident solar flux depends only weakly on ν. In this case we can approximate (2.6) by

$$W(\mu, \varphi) = \int_{\Delta\nu} [1 - S_\nu(\mu, \varphi; \mu_0\varphi_0)/S_\infty(\mu, \varphi; \mu_0\varphi_0)]\, d\nu \tag{2.7}$$

or, if

$$R_\nu(\bar{\mu}) = I_\nu(\bar{\mu})/F_\nu$$

where $I_\nu(\bar{\mu})$ is defined by (2.2), then

$$W(\bar{\mu}) = \int_{\Delta\nu} [1 - R_\nu(\bar{\mu})/R_\infty(\bar{\mu})]\, d\nu. \tag{2.8}$$

We shall use expressions (2.7) and (2.8) to compare with the observational data.

II.3 *Calculation of the Coefficient of Diffuse Reflection*

The coefficient of diffuse reflection can be derived most conveniently as the solution of an initial-value problem. It satisfies the equation

$$\begin{aligned} &\frac{\partial}{\partial\tau} S_\nu(\mu, \mu_0; \tau) + \left(\frac{1}{\mu} + \frac{1}{\mu_0}\right) S_\nu(\mu, \mu_0; \tau) \\ &= \tilde{\omega}_\nu(\tau) \left\{1 + \frac{1}{2} \int_0^1 S_\nu(\mu, \mu'; \tau) \frac{d\mu'}{\mu'}\right\} \left\{1 + \frac{1}{2} \int_0^1 S_\nu(\mu'', \mu_0; \tau) \frac{d\mu''}{\mu''}\right\}, \end{aligned} \tag{2.9}$$

$0 < \mu, \mu_0 \leq 1$, $0 \leq \tilde{\omega}_\nu(\tau) \leq 1$, with $S_\nu(\mu, \mu_0; 0)$ given. In this equation, $S_\nu(\mu, \mu_0; \tau)$ represents the coefficient of a diffuse reflection for a plane slab of normal optical thickness τ. The albedo for single scattering, $\tilde{\omega}_\nu(\tau)$, is the ratio of the scattering cross section of the medium to the total cross section, and is in general a function of position within the slab. Equation (2.9) can be derived most simply by considering the change in $S_\nu(\mu, \mu_0; \tau)$ arising from the addition of a layer of optical thickness $\delta\tau$ at the top of the slab and allowing $\delta\tau$ to tend to zero. The derivation is well-known [4], [5], [6], and will not be given here. Busbridge [5], demonstrates that for any $\tilde{\omega}_\nu(\tau)$ satisfying $0 \leq \tilde{\omega}_\nu(\tau) \leq \tilde{\omega}_1 < 1$, Eq. (2.9) has a solution.

III. Numerical Solution of the Diffuse Reflection Problem

The simplest way of deriving an approximate solution of (2.9) for a fixed value of ν is to replace the integro-differential equation by a set of simultaneous ordinary differential equations,

$$\frac{d}{d\tau} S_{ij}(\tau) + \lambda_{ij} S_{ij}(\tau) = \tilde{\omega}_\nu \varphi_i(\tau)\varphi_j(\tau), \tag{3.1}$$

where $\lambda_{ij} = \mu_i^{-1} + \mu_j^{-1}$,

$$S_{ij}(\tau) \approx S_\nu(\mu_i, \mu_j; \tau), \qquad 1 \leq i, j \leq N, \tag{3.2}$$

and

$$\varphi_i(\tau) \approx \varphi(\tau, \mu_i) = 1 + \frac{1}{2} \int_0^1 S_\nu(\mu_i, u; \tau) \frac{du}{u}, \tag{3.3}$$

$1 \leq i \leq N$. The μ_i form a partition of [0, 1],

$$\mu_0 = 0 < \mu_1 < \ldots < \mu_N = 1.$$

The set of functions $S_{ij}(\tau)$ is obviously symmetrical in i and j,

$$S_{ij}(\tau) = S_{ji}(\tau)$$

and for $0 \leq i \leq N$

$$S_{i0}(\tau) = S_{0i}(\tau) = 0, \text{ and } \varphi_0(\tau) = 1.$$

The boundary conditions prescribe $S_{ij}(\tau)$ at $\tau = 0$ for all values of i and j.

The accuracy with which $S_{ij}(\tau)$ approximates $S_\nu(\mu_i, \mu_j; \tau)$ clearly depends on two things: the process used to derive approximate solutions of (3.1), and the quadrature formula used to approximate the right-hand side of (3.3) in terms of members of the array $S_{ij}(\tau)$. We dispose of the former first. On the Atlas computer, solution of simultaneous ordinary differential equations such as (3.1) is conveniently handled by a FORTRAN library routine for the Runge-Kutta–Merson process [7], [8]. This subroutine provides an error estimate which permits us to control the step-length $\Delta\tau$. This depends slightly on the value of N, and we have found that the estimated local truncation error when $N = 8$ is at worst 10^{-5} or 10^{-6} with $\Delta\tau \sim 0.1$, quite a large enough step for practical purposes.

The method of quadrature to be used in approximating the right-hand side of (3.3) presents a much more serious problem. In choosing such a quadrature formula, we need to assess both its accuracy and suitability for the job. We could, for example, follow Bellman *et al.* [6] and employ Gauss–Legendre quadrature of order N. Although this gives an efficient approximation to $\varphi(\tau, \mu_i)$, it makes it difficult to compute the emergent intensity from (2.2) since we do not know how to reconstruct the underlying Hermite interpolation polynomial without knowledge of the derivatives at the integration points. Calculation of (2.2) would still be difficult, even if we had this information, because of the high order of the interpolation polynomial.

For this reason, we have chosen to use a quadratic spline to interpolate between pivotal values of μ. This provides simplicity of calculation with accuracy little inferior to that of the Gauss–Legendre quadrature in this application. The spline is completely defined by the values of the function at the joints μ_i, $i = 0, 1, \ldots, N$, by the requirement that the spline have a continuous gradient at each joint, and by a boundary condition. Now as $\mu' \to 0$, it is not difficult to show that

$$S_\nu(\mu, \mu'; \tau) \approx \tilde{\omega}_\nu(\tau) \frac{\mu\mu'}{\mu + \mu'} \varphi(\tau, \mu) \left\{1 + \frac{1}{2} \tilde{\omega}_\nu(\tau)\mu \ln \left(\frac{\mu' + 1}{\mu'}\right) + \ldots\right\} \quad (3.4)$$

so that

$$\frac{\partial}{\partial\mu'} S_\nu(\mu, \mu'; \tau) \to \tilde{\omega}_\nu(\tau)\, \varphi(\tau, \mu) \text{ as } \mu' \to 0.$$

Thus (3.4) provides a suitable boundary condition.
We now define for a fixed value of μ

$$f(\mu') = S_\nu(\mu, \mu'; \tau),\ f_k = f(\mu_k) \qquad (k = 0, 1, \ldots, N) \quad (3.5)$$

and a quadratic spline $\Phi(f; \mu)$ approximating $f(\mu)$,

$$\Phi(f;\mu) = \Phi_{k+1/2}(f;\mu) \begin{cases} \mu_k \leq \mu \leq \mu_{k+1}, \\ 0 \leq k \leq N-1, \end{cases} \tag{3.6}$$

where, if $l_{k+1/2} = \mu_{k+1} - \mu_k$,

$$\Phi_{k+1/2}(f;\mu) = \frac{(\mu-\mu_k)f_{k+1} + (\mu_{k+1}-\mu)f_k}{l_{k+1/2}} - g_{k+1/2}\frac{(\mu_{k+1}-\mu)(\mu-\mu_k)}{l_{k+1/2}^2}.$$

Clearly,

$$\Phi_{k+1/2}(f;\mu_k) = f_k, \quad \Phi_{k+1/2}(f;\mu_{k+1}) = f_{k+1}$$

as required, and the condition

$$\frac{d}{d\mu}\Phi_{k+1/2}(f;\mu) = \frac{d}{d\mu}\Phi_{k-1/2}(f;\mu), \ \mu = \mu_k \tag{3.7}$$

can be satisfied if

$$\frac{g_{k+1/2}}{l_{k+1/2}} + \frac{g_{k-1/2}}{l_{k-1/2}} = \frac{f_{k+1}-f_k}{l_{k+1/2}} - \frac{f_k - f_{k-1}}{l_{k-1/2}} \tag{3.8}$$

for $1 \leq k \leq N-1$. If we provide a boundary condition to determine $g_{1/2}$, say, these equations define $g_{k+1/2}$ uniquely for $1 \leq k \leq N-1$. We choose

$$f_0' = \Phi_{1/2}'(f;\mu)$$

at $\mu = 0$, giving

$$g_{1/2} = f_1 - f_0 - l_{1/2}f_0'. \tag{3.9}$$

The truncation error, defined by

$$R_{k+1/2}(f;\mu) = f(\mu) - \Phi_{k+1/2}(f;\mu)$$

is studied in Appendix B. For the important case in which the joints are uniformly spaced ($l_{k+1/2} = N^{-1} = l$ for all k), we have

$$\begin{aligned} R_{2m+1/2}(f;\mu) &= -\tfrac{1}{6}\theta^2(1-\theta)l^3 f_{2m}''' + \ldots, \\ R_{2m+3/2}(f;\mu) &= +\tfrac{1}{6}\theta(1-\theta)^2 l^3 f_{2m+1}''' + \ldots, \end{aligned} \qquad m = 0, 1, 2, \ldots. \tag{3.10}$$

where $\theta = (\mu - \mu_k)/l$, $0 \leq \theta \leq 1$. In our case, f_0''' does not exist, but for the purposes of (3.10) we define $f_0''' = f_1'''$. Thus

$$|R_{k+1/2}(f;\mu)| < \frac{2Ml^3}{81} \quad k = 0, 1, \ldots,$$

where $M = \sup_k |f_k'''|$.

We insert (3.6) into the right-hand side of (3.3), and, after eliminating f_0' with (3.4) we arrive at the approximation

$$\varphi_i(\tau) = \frac{1}{1 - \frac{1}{2}\tilde{\omega}_r(\tau)\Delta} + \frac{1}{2}\sum_{k=1}^{N} c_k(\tau) S_{ki}(\tau), \tag{3.11}$$

for $1 \leq i \leq N$, $\varphi_0(\tau) = 1$. The coefficients $c_k(\tau)$ are defined by

$$c_k(\tau) = c_k^{(1)} + c_k^{(2)}(\tau)$$

where

$$c_1^{(1)} = \frac{\mu_2}{l_{3/2}} \ln\left(\frac{\mu_2}{\mu_1}\right),$$

$$c_k^{(1)} = \frac{\mu_{k+1}}{l_{k+1/2}} \ln\left(\frac{\mu_{k+1}}{\mu_k}\right) - \frac{\mu_{k-1}}{l_{k-1/2}} \ln\left(\frac{\mu_k}{\mu_{k-1}}\right), \quad k = 2, 3, \ldots, N-1,$$

$$c_N^{(1)} = 1 - \frac{\mu_{N-1}}{l_{N-1/2}} \ln\left(\frac{\mu_N}{\mu_{N-1}}\right),$$

and

$$c_1^{(2)}(\tau) = \left\{\frac{1}{2}\left[\frac{1}{2}\tilde{\omega}_r(\tau)\Delta \cdot c_1^{(1)} - d_1\right] - \frac{1}{2}\frac{\Delta}{l_{1/2}}\right\} \Big/ \left[1 - \frac{1}{2}\tilde{\omega}_r(\tau)\Delta\right]$$

$$c_k^{(2)}(\tau) = \tfrac{1}{2}[\tfrac{1}{2}\tilde{\omega}_r(\tau)\,\Delta \cdot c_k^{(1)} - d_k] \,/\, [1 - \tfrac{1}{2}\tilde{\omega}_r(\tau)\,\Delta], \quad k = 2, 3, \ldots, N$$

where, if

$$l_{k+1/2}h_{k+1/2} = \int_{\mu_k}^{\mu_{k+1}} (\mu_{k+1} - \mu)(\mu - \mu_k)\frac{d\mu}{\mu},$$

$$\Delta = \sum_{k=0}^{N-1} (-1)^k h_{k+1/2},$$

$$d_k = \frac{e_{k-1/2}}{l_{k-1/2}} - \frac{e_{k+1/2}}{l_{k+1/2}}, \quad k = N, N-1, \ldots, 1,$$

$$e_{N+1/2} = 0, \; e_{N-1/2} = h_{N-1/2}, \; e_{k-1/2} = h_{k-1/2} - (h_{k+1/2} + e_{k+1/2})$$

for $k = (N-1), (N-2), \ldots, 2$ in succession, and $e_{1/2} = -\frac{1}{2}(e_{3/2} + h_{3/2})$.

Using (3.10), we can estimate a bound for the error functional

$$R^*(\varphi; \mu_i) = \varphi(\tau, \mu_i) - \varphi_i(\tau)$$

and we find

$$|\, R^*(\varphi; \mu_i)\,| < \frac{Ml^2}{48}. \tag{3.12}$$

We are now in a position to estimate how the truncation error is propagated by the differential equations (3.1). These may be integrated formally to give the solution

$$S_{ij}(\tau) = \exp(-\lambda_{ij}\tau)S_{ij}(0) + \int_0^\tau \exp[-\lambda_{ij}(\tau - t)]\,\tilde{\omega}_\nu(t)\varphi_i(t)\varphi_j(t)\,dt. \quad (3.13)$$

If $S_{ij}(0)$ is exact, the error $\sigma_{ij}(\tau)$ in $S_{ij}(\tau)$ is given to lowest order by

$$\sigma_{ij}(\tau) = \int_0^\tau \exp[-\lambda_{ij}(\tau - t)]\,\tilde{\omega}(t)[\varphi_i(t)R^*(\varphi;\mu_j) + \varphi_j(t)R^*(\varphi;\mu_i)]\,dt$$

and so, using (3.12).

$$\begin{aligned} |\,\sigma_{ij}(\tau)\,| &\leq \frac{Ml^2}{24}\,\bar{\varphi}\int_0^\tau \exp[-\lambda_{ij}(\tau - t)]\,dt \\ &< \frac{\mu_i\mu_j}{\mu_i + \mu_j}\,\frac{M\bar{\varphi}}{24}\cdot l^2, \end{aligned} \quad (3.14)$$

where $\bar{\varphi}$ is a uniform bound for $\varphi_i(\tau)$. We therefore expect the truncation error in the solution $S_{ij}(\tau)$ to converge as $(1/N^2)$.

IV. Numerical Computation of Reflected Intensities

We can use the interpolating spline (3.6) to write down approximations for reflected intensities. Thus the intensity of radiation reflected from the planet at a given phase angle can be written as in (2.2),

$$I_\nu(\bar{\mu}) = \frac{F_\nu}{2\pi}\int_0^1 s(\mu)\,d\mu, \quad (4.1)$$

where, for an isotropic scattering atmosphere

$$s(\mu) = \int_{m(\mu,\bar{\mu})}^{M(\mu,\bar{\mu})} \frac{S_\nu(\mu,\mu')\,d\mu'}{[1 - \mu^2 - \mu'^2 - \bar{\mu}^2 + 2\mu\mu'\bar{\mu}]^{1/2}} \quad (4.2)$$

Now using (3.5) and (3.6) we find

$$s(\mu) \approx s^{(1)}(\mu) + s^{(2)}(\mu)$$

where

$$s^{(1)}(\mu) = \sum_{j=1}^{N} C_j^{(1)}(\mu)\,f_j\,, \qquad s^{(2)}(\mu) = \sum_{j=1}^{N-1} C_{j+1/2}^{(2)}(\mu)\,g_{j+1/2}. \quad (4.3)$$

We tabulate the functions f_j, $\varphi_i(\tau)$, so that the $g_{j+1/2}$ can be determined from (3.8), (3.9), and (3.4). If μ is not one of the values of μ_i at which the solution is given, we use (3.5) and (3.6) to set up the values of f_j.

The coefficients are defined as follows:

$$C_j^{(1)}(\mu) = A_{j+1/2}(\mu) + B_{j-1/2}(\mu) \; (1 \leq j \leq N) \tag{4.4}$$

where

$$\begin{aligned}
A_{j+1/2}(\mu) &= [(\mu_{j+1/2} - \mu\bar{\mu})P_{j+1/2} - Q_{j+1/2}] \,/\, l_{j+1/2} \quad (1 \leq j \leq N-1) \\
&= 0 \qquad\qquad\qquad\qquad\qquad\qquad\qquad\quad (j = N), \\
B_{j+1/2}(\mu) &= [-(\mu_j - \mu\bar{\mu})P_{j+1/2} + Q_{j+1/2}] \,/\, l_{j+1/2} \quad (1 \leq j \leq N), \\
P_{j+1/2} &= \Theta(\mu_{j+1}) - \Theta(\mu_j), \\
Q_{j+1/2} &= \Phi(\mu_{j+1}) - \Phi(\mu_j),
\end{aligned}$$

$$\Theta(u) = \begin{cases} -\pi/2 & \text{if } u \leq m(\mu,\bar{\mu}) \\ \sin^{-1}\left\{\dfrac{u - \mu\bar{\mu}}{[(1-\mu^2)(1-\bar{\mu}^2)]^{1/2}}\right\} & \text{if } m(\mu,\bar{\mu}) \leq u \leq M(\mu,\bar{\mu}), \\ \pi/2 & \text{if } u \geq M(\mu,\bar{\mu}) \end{cases}$$

$$\Phi(u) = \begin{cases} -[1 - \bar{\mu}^2 - \mu^2 - u^2 + 2\mu\bar{\mu}u]^{1/2} & \text{if } m(\mu,\bar{\mu}) \leq u \leq M(\mu,\bar{\mu}) \\ 0 & \text{otherwise} \end{cases}$$

Also, for $0 \leq j \leq N-1$,

$$\begin{aligned}
C_{j+1/2}^{(2)}(\mu) = \{&[\tfrac{3}{2}\mu^2\bar{\mu}^2 - \tfrac{1}{2}\mu^2 - \tfrac{1}{2}\bar{\mu}^2 + \tfrac{1}{2} - \mu\bar{\mu}(\mu_j + \mu_{j+1}) + \mu_j\mu_{j+1}]P_{j+1/2} \\
&+ [\tfrac{3}{2}\mu\bar{\mu} - \mu_j - \mu_{j+1}]Q_{j+1/2} + \tfrac{1}{2}R_{j+1/2}\} \,/\, l_{j+1/2}^2
\end{aligned} \tag{4.5}$$

where

$$R_{j+1/2} = \mu_{j+1}\Phi(\mu_{j+1}) - \mu_j\Phi(\mu_j).$$

In special cases the formulas simplify. When $\mu = 1$, $\mu_J \leq \bar{\mu} \leq \mu_{J+1}$, we have $Q_{j+1/2} = R_{j+1/2} = 0$ for all j, $P_{j+1/2} = 0$ when $j \neq J$, and $P_{J+1/2} = \pi$. Thus, in terms of the interpolating spline (3.6) we have

$$s(1) = \pi\,\Phi_{J+1/2}(f;\bar{\mu}). \tag{4.6}$$

Similarly, when $\bar{\mu} = 1$, $\mu_J \leq \mu \leq \mu_{J+1}$,

$$s(\mu) = \pi\,\Phi_{J+1/2}(f;\mu). \tag{4.7}$$

Once we have $s(\mu)$, the quadrature (4.1) can be performed by any convenient

method. We find that the trapezoidal rule gives at least two significant figures, which is adequate for our purposes.

We can calculate the plane albedo, defined by (2.5) in a similar way. With $f(\mu) = S_\nu(\mu, \mu_0; \tau)$ for fixed μ_0, we have

$$a_\nu(\mu_0) = \frac{1}{2\mu_0} \sum_{j=0}^{N-1} l_{j+1/2} \left[\frac{1}{2} (f_j + f_{j+1}) - \frac{1}{6} g_{j+1/2} \right]. \tag{4.8}$$

The spherical albedo can be computed from (4.8) by approximating to

$$A_\nu = \int_0^1 2\mu_0 a_\nu(\mu_0)\, d\mu_0$$

with the trapezoidal rule.

V. Simple Model Atmospheres

We now list the specific assumptions needed to construct our atmospheric model.

V.1 *Hydrostatic Equilibrium*

The condition of hydrostatic equilibrium is expressed by the equation

$$dp = -g\varrho\, dz, \tag{5.1}$$

where p is pressure, g the acceleration due to gravity, and ϱ the density at height z above the planetary surface.

V.2 *Composition*

We assume uniform composition. Let ϱ_i be the density of constituent i, $\varrho = \Sigma \varrho_i$. Then the fraction of constituent i by mass is

$$\begin{gathered} r_i = \varrho_i/\varrho \text{ (a constant)}, \\ \Sigma\, r_i = 1. \end{gathered} \tag{5.2}$$

Similarly, if μ_i is the molecular weight of constituent i, the fraction of i present by number (or volume) is

$$\begin{aligned} s_i &= (\varrho_i/\mu_i) \,/\, (\varrho/\mu) \text{ (a constant)}, \\ \mu &= \varrho/(\Sigma\, \varrho_i/\mu_i),\ \Sigma\, s_i = 1. \end{aligned} \tag{5.3}$$

If there are only two gases, there is a particularly simple relation between $r(=r_1)$ and $s(=s_1)$, namely

$$s = r/\left[r + \frac{\mu_1}{\mu_2}(1 - r)\right]. \tag{5.4}$$

The equation of state is assumed to be

$$p = \varrho\, RT/\mu. \tag{5.5}$$

V.3 *Height Variation of Temperature*

The variation of temperature is determined by the heat balance in the atmosphere together with the equation of state and the equation of hydrostatic equilibrium, and thus can only be obtained *ab initio* by solving a complex radiative transfer problem, for which we have no data. For our purposes, we shall assume a uniform lapse rate of temperature

$$T = T_0\left[1 - \frac{z - z_0}{L}\right] \tag{5.6}$$

where T_0 is the temperature at some pivotal height z_0, and L is a characteristic height.

V.4 *Dependence of Other Physical Parameters on Height*

Using (5.1), (5.5), (5.6), and the relation

$$g = g_0\left[1 - \frac{z - z_0}{a}\right]^{-2} \tag{5.7}$$

expressing the variation of gravity with height (a is the radius of a sphere concentric with the planet at height z_0 above the surface), we can obtain a a relation between p and z, namely

$$\frac{p}{p_0} = \left[\frac{1 - (z - z_0)/L}{1 + (z - z_0)/a}\right]^{\gamma} \exp\left[-\frac{\gamma}{a}\,\frac{(z - z_0)(a + L)}{a + (z - z_0)}\right], \tag{5.8}$$

where

$$\gamma = (L/H)(1 + L/a)^{-2},$$

$$H = RT_0/\mu g_0.$$

To the order of accuracy needed we have $| z - z_0 |$, $L \ll a$, so that

$$\begin{aligned} T/T_0 &= (p/p_0)^{1/\gamma}, \\ \varrho/\varrho_0 &= (p/p_0)^{1-1/\gamma}, \\ z &= z_0 + L(1 - T/T_0). \end{aligned} \tag{5.9}$$

V.5 *Tabulation of Atmospheric Parameters*

It is convenient to use the following units:

Pressure:	mb $\equiv 10^3$ dyne/cm^2
Temperature:	°K
Height:	km $\equiv 10^5$ cm
Density:	g/cm^3
Frequency:	cm^{-1}.

As the fundamental parameters of the model we take

(i) Scale height: H (km)
(ii) Scale height for temperature: L (km)
(iii) Effective gravity: g_0 (cm/sec^2)
(iv) Pivotal pressure: p_0 (mb)
(vi) Ground temperature: T_g (°K).

Then we can easily derive the remaining parameters:

$$\begin{aligned} \gamma &= L/H \\ \mu &= (RT_0/gH) \times 10^{-5} \text{ g/mole} = 831.7\,(T_0/gH) \text{ g/mole}, \\ \varrho_0 &= 10^{-2}\, p_0/gH \quad \text{g/cm}^3 \\ p_g &= p_0(T_g/T_0)^{\gamma}, \end{aligned}$$

after which the distributions (5.9) can be evaluated.

V.6 *Optical Depth Calculation—Venus*

At this point we must make a more definite assumption about the constitution of the Venus atmosphere. We assume that there are only two constituents of

importance, namely CO_2 (constituent 1) and N_2. We assume that the main absorption of radiation near the λ-7820 CO_2 band is due to the band itself and that N_2 is transparent. There is a material present which scatters radiation and which is uniformly mixed in the atmosphere. There may be a small residual background absorption in the wings of the lines due to materials other than CO_2.

We compute the CO_2 absorption from the formula

where ν_J is the central frequency of the Jth line, β depends on the rotational energy constant B by $\beta = Bhc/kT_0$ ($Bhc/k = 0.5614$°K for CO_2), and K_0 measures the band strength. The factor $g_J = J$ for the P-branch [$\nu_J = \nu_0 - 2BJ$] and $J + 1$ for the R-branch [$\nu_J = \nu_0 + 2B(J + 1)$]. The linewidth α is given by

$$\alpha = \alpha_0 \left(\frac{p}{p_0}\right) \left(\frac{T_0}{T}\right)^{1/2} \tag{5.11}$$

where [3]

$$\alpha_0 = 10^{-3} p_0 \left(\frac{300}{T_0}\right)^{1/2} (0.07 + 0.03s)$$

with s obtained from (5.4) as

$$s = 7r/(11 - 4r)$$

for a binary mixture of CO_2 and N_2.

For convenience we now introduce the notation $x = p/p_0$, $y = T_0/T = x^{-1/\gamma}$, $u_J = (\nu - \nu_J)/\alpha_0$, and assume that the lines do not overlap. Then

$$K_\nu = (K_0 g_J/\pi\alpha_0) \exp[-\beta J(J + 1)y] \left[\frac{xy^{3/2}}{u_J^2 + x^2 y}\right]. \tag{5.12}$$

If σ is the scattering cross section and $\tilde{\omega}_0$ the albedo in the wings of the line (nearly unity), then the single-scattering albedo is

$$\begin{aligned}\tilde{\omega}_J(u_J, x) &= \frac{\sigma}{rK_\nu + (\sigma/\tilde{\omega}_0)} \\ &= \left\{\tilde{\omega}_0^{-1} + \left(\frac{\bar{\tau}}{\bar{t}}\right)\left(\frac{g_J}{\pi\alpha_0}\right) \exp[-\beta_J(J + 1)y] \left[\frac{xy^{3/2}}{u_J^2 + x^2 y}\right]\right\}^{-1}\end{aligned} \tag{5.13}$$

where $\bar{\tau} = 10^3\ (rK_0)$, and $\bar{t} = 10^3\,\sigma$. The optical depth at this frequency is defined by the equation

$$d\tau = -[rK_J + (\sigma/\tilde{\omega}_0)]\,\varrho\,dz$$

$$= -\frac{\sigma\varrho\,dz}{\tilde{\omega}_J(u_J, x)}$$

$$= \frac{\bar{t}\,dp}{\tilde{\omega}_J(u_J, x)}$$

$$= \frac{p_0\bar{t}}{\tilde{\omega}_J(u_J, x)}\,dx. \tag{5.14}$$

This equation, regarded either as a differential equation for τ in terms of x or for x in terms of τ, can be solved by the same Runge-Kutta procedure as are the invariant imbedding equations (3.1).

The preceding equations make it clear that the ratio $\bar{t}/\bar{\tau}$, which is unknown, controls the variation of the albedo for single scattering with height and that $\bar{t}$ controls the overall optical thickness of the atmosphere in the wings of the line. Thus if we fix the parameters listed in Section V.5, the albedo of the planet far from line centers fixes $\bar{t}$, and the equivalent width of the absorption lines fixes $\bar{\tau}$. Since $\bar{\tau} = 10^3(r\,K_0)$, this determines the relative abundance r, provided K_0 is known. Kaplan (private communication) has quoted the equivalent width of the $J = 16$ line for a path length of 8-km-atm. CO_2 at around 300°K as 40 mA (0.06 cm^{-1}). This gives the value

$$K_0 = 2.5 \times 10^{-3}\,\beta\ \mathrm{cm^2/g\ cm}\,. \tag{5.15}$$

which we have used in our runs.

VI. The Snark and Snark Editor Codes

The principles guiding the construction of these codes were laid down in the introduction. Block diagrams of the codes are set out in Figs. 1 and 2. The procedure is dictated, to some extent, by certain features of the Ampex magnetic tape system connected to the Science Research Council's Atlas computer at Chilton. The codes as a whole have been written in the local FORTRAN language (HARTRAN) with the exception of three subroutines for handling magnetic tapes. The most efficient way of transmitting information to and from magnetic tape is to work with blocks of a fixed length of 512 words. Blocks on the tape are individually addressable, so that it is possible to write an index at the beginning of the tape describing the current state of the computation at the end of every run, thus

facilitating restarts with a minimum of manual intervention. Output of data to magnetic tape and its subsequent retrieval is buffered by blocks.

With these remarks, the rest of Fig. 1 is almost self-explanatory. The running instruction parameter NACT defines the initial action of the program. To read

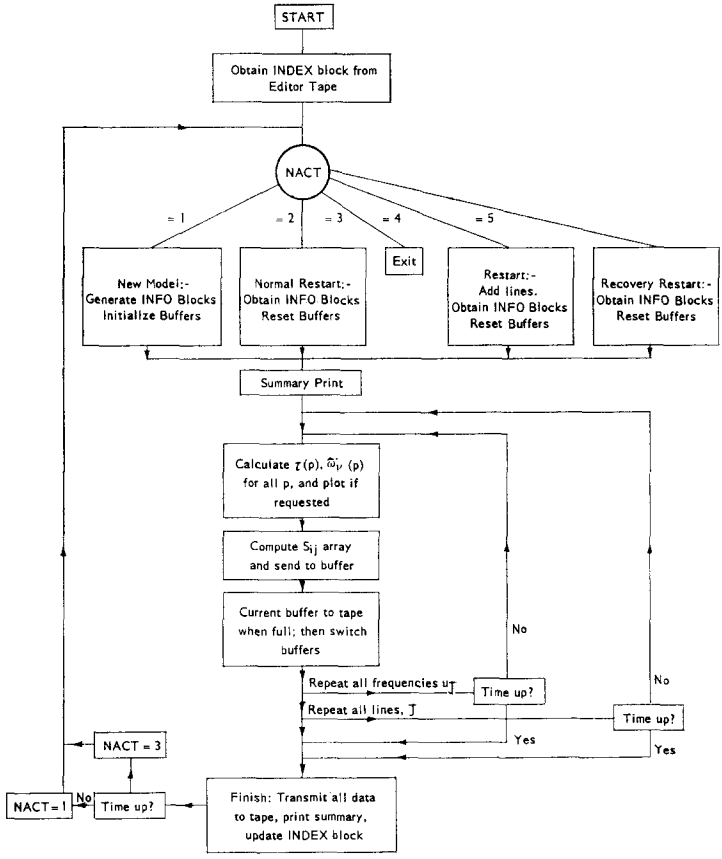

FIG. 1. SNARK code. Simplified flow diagram.

in data for a new model we set NACT = 1. The code then sets up all the basic information needed, including the constants $c_k^{(n)}$ of (3.11) and the tabulation of Section V.5, and transmits the whole of this data (2 blocks) to magnetic tape. It also prepares the buffers in which the matrices S_{ij} are to be stored. The option NACT = 2 permits a restart from the position reached in a previous session on the machine. The basic data are retrieved from tape, the contents of the buffers

at termination of the last session are reconstituted, and calculation proceeds from there. In a similar way we use NACT = 4 to permit a restart specifying additional lines to be computed, and NACT = 5 to allow us to go back to where an error occurred. The option NACT = 3 terminates the session.

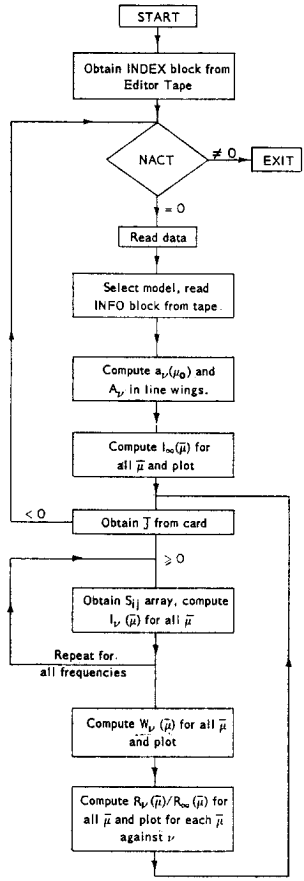

FIG. 2. SNARK EDITOR code. Simplified flow diagram.

The main computing loop consists of a cycle in which we first of all specify values of J and u_J, and then use (5.14) to tabulate x and $\tilde{\omega}_J(u_J, x)$ for a suitable distribution of values of τ. Then we solve Equations (3.1) using (3.11), as described, to obtain $S_{ij}(\tau)$ at the top of the atmosphere. When complete the array $S_{ij}(\tau)$ is stored in the buffer and transmitted to tape when the buffer is filled. We can also arrange for tables of $\tau(u_J)$ and $\tilde{\omega}_J(u_J, x)$ against $\log p(x)$ to be transmitted

to an automatic graph-plotter via IBM ½-in. magnetic tape. The cycle continues until we have exhausted all pairs of values of J and u_J.

The SNARK EDITOR code (Fig. 2) extracts information from the magnetic tape and computes $a_\nu(\mu_0)$, A_ν and $I_\nu(\bar{\mu})$ as described in Section IV. Some of the information, such as equivalent widths and albedos, is printed, the remainder transmitted to graph-plotter, so that we obtain graphs of $I_\nu(\bar{\mu})$ far from line centers, and $R_\nu(\bar{\mu})$ against ν automatically. For an isolated line we must estimate the contribution to the equivalent width from the far wings outside the tabulated range of u_J. We fit the tail of the line by an expression of the form

$$\left[1 - \frac{R_\nu(\bar{\mu})}{R_\infty(\bar{\mu})}\right] \approx (a + b \mid u_J \mid + c \mid u_J \mid^2)^{-1}$$

whose contribution is easily evaluated.

VII. Tests and Specimen Calculations

Our first use of the program has been to study the validity of the numerical method. We have examined the accuracy and convergence of our solutions for the case of conservative scattering ($\tilde{\omega}_\nu(\tau) = 1$), and we have compared our results with other published solutions, notably those of Bellman *et al.* [6]. Starting with the initial conditions $S_{ij}(0) = 0$, we integrated the equations (3.1) over the range $0 \leq \tau \leq 6.3$ in steps of 0.1. We took for simplicity a uniform distribution of μ-values, with l taking values of 0.25, 0.125, and 0.1 ($N = 4$, 8, 10).

To begin with, the truncation error estimate provided by the Runge-Kutta-Merson subroutine was always small. It was largest in the first step from $\tau = 0$ to 0.1. At this point it was 1.4×10^{-5} for $N = 4$, and fell rapidly to order 10^{-9} for $\tau \sim 3$. The accuracy demanded was 10^{-4}, so that it was never necessary to cut the step size. The behavior for larger values of N was similar, although it was necessary to halve the step size for the first three intervals for $N = 8$ and 10. This is to be expected because of the increase in $\max[\lambda_{ij}] = \lambda_{11}$ as N increases.

Next, let us consider the question of convergence and of quadrature errors. For ease of comparison with the solution of Bellman *et al.* [6], we choose the only integration point which is common to the two integration schemes, namely $\mu = \mu_0 = 0.5$, at $\tau = 6.3$. The numerical solutions for the diffuse reflection coefficient $S(0.5, 0.5; 6.3)$ are shown in Table I. The line labeled SNARK 2 contains values calculated from the quadratic spline formulas, and that labeled SNARK 1 assumes only a linear variation between joints. The SNARK 2 values converge much more rapidly with N, and it is clear that this is a greatly superior approxi-

TABLE I

NUMERICAL VALUES OF $S(0.5, 0.5; 6.3)$ WHEN $\tilde{\omega}(\tau) = 1$ FOR ALL τ.

N	4	8	10	Limit
SNARK 2	0.8647	0.8769	0.8785	0.8811 ± 0.0002
SNARK 1	0.8085	0.8586	0.8661	—

mation. The error estimate (3.14) has been used to extrapolate to the limit as $N \to \infty$; taking the SNARK 2 values for different N in pairs, we find a limiting value around 0.8811, wtih an uncertainty of about 0.0002. This is in fair agreement with the figure of 0.88164 quoted by Bellman *et al.* [6], who used 7-point Gauss–Legendre quadrature. Our solution with $N = 8$ appears to be in error by not more than $\frac{1}{2}\%$, which is quite good enough for our purposes, and we have adopted $N = 8$ as standard in all our production calculations. The behavior for other values of μ, μ_0 and τ is comparable.

As an example of a practical calculation done with the code we have computed an atmosphere whose basic parameters are listed in Table II. This is essentially

TABLE II

MODEL ATMOSPHERE PARAMETERS

Scale height H	7.423 km
Temperature Scale Height L	48.454 km
Effective gravity g_0	890 cm/sec^2
Pivotal temperature T_0	230°K
Ground temperature T_g	700°K
Pivotal pressure p_0	7 mb
Derived parameters	
$\gamma = L/H = 6.5275$	$\mu = 28.96$
$\varrho_0 = 1.05 \times 10^{-5}$ g/cm^3	$p_g = 10^4$ mb
Optical parameters	
$K_0 = 6.102 \times 10^{-6}$ cm^{2}g^{-1}/cm^{-1}	
$\alpha_0 = 5.918 \times 10^{-4}$ cm^{-1} (corresponding to CO_2 mixing ratios $r = 0.2$ by mass, $s = 0.14$ by volume)	
$\tilde{\omega} = 0.985$	
$\bar{t}/\bar{\tau} = 500$	

the "standard" atmosphere proposed by Kaplan [9] with the exception that we [illegible] although we have varied the CO_2 mixing ratio s from his value of 10%. The effect of this inconsistency is small. The value of $\tilde{\omega}_0$ has been chosen so that the planetary albedo far from the line center, A_ν (Table III) is computed to be about 75%. We have assumed all radiation reaching

TABLE III

PLANE ALBEDO $\tilde{\omega}_0 = 0.985$, $S(\mu, \mu_0 ; 0) = 0$

μ_0 =	.125	.250	.375	.500	.625	.750	.875	1.000
$a_\nu(\mu_0)$ =	.834	.807	.782	.760	.738	.718	.699	.681

Spherical Albedo $A_\nu = .734$

the surface of the planet is absorbed. A value $\tilde{\omega}_0 = 1.0$ makes the planetary albedo considerably larger, 82%. It is clear that we could not allow $\bar{t}$ to change much without making drastic changes to the value of A_ν.

The dependence of τ and $\tilde{\omega}_\nu$ on pressure is shown in Figs. 3, 4, and 5 for three different frequencies in the $J = 18$ line profile. Figure 4 refers to the line center, Fig. 5 to the maximum value of $| \nu - \nu_J |$ that was computed (500 α_0), and Fig. 3

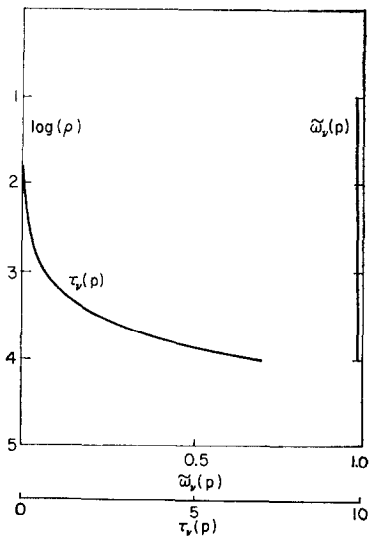

FIG. 3. Variation of albedo and optical depth, with logarithm of pressure as ordinate, far from the line center.

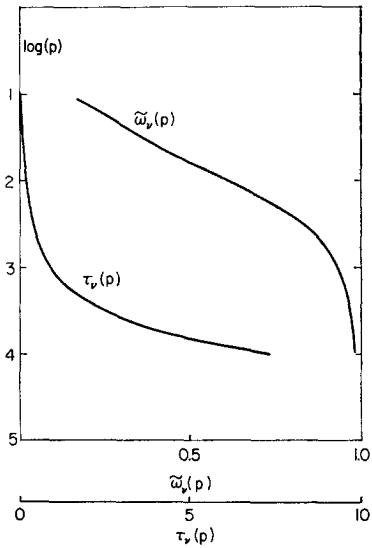

FIG. 4. Variation of albedo and optical depth, with logarithm of pressure as ordinate, for the centre of the $J = 18$ line.

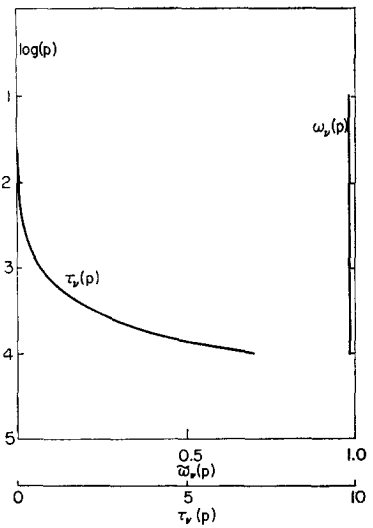

FIG. 5. Variation of albedo and optical depth, with logarithm of pressure as ordinate, in the wing of the $J = 18$ line, $|\nu - \nu_{18}| = 0.3018\ \text{cm}^{-1}$.

to $|\nu - \nu_J| \to \infty$, where the albedo for single scattering has the constant value $\tilde{\omega}_0$ at all levels in the atmosphere. This provides us with a standard of intensity $I_\infty(\bar{\mu})$ whose variation with $\bar{\mu}$ is shown in Fig. 6. The phase dependence of the equivalent width of the line $W(\bar{\mu})$ is shown in Fig. 7, and a selection of line profiles,

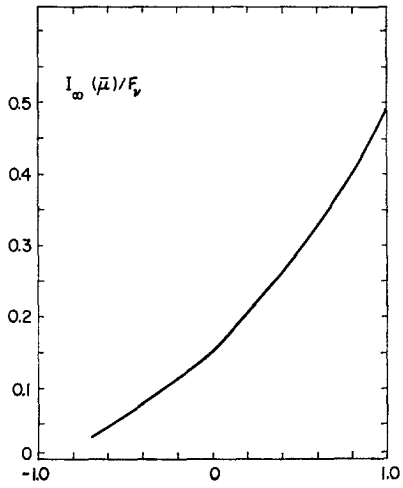

FIG. 6. Diffusely reflected specific intensity, $I_\infty(\bar{\mu})F_\nu$ versus $\bar{\mu}$ far from the line center.

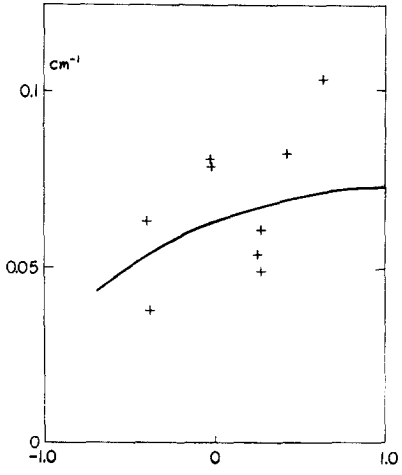

FIG. 7. Equivalent width for the $J = 18$ line vs. $\bar{\mu}$. The crosses represent observed values quoted by Spinrad [3] in his Table I. One of his points at $\bar{\mu} = 0.391$ lies off scale at 0.136 and is therefore not shown.

$R_\nu(\bar{\mu})/R_\infty(\bar{\mu})$, are given in Fig. 8 for various values of the cosine of the phase angle. We intend to discuss elsewhere the physical implications of our calculations, of which these results form a sample.

The SNARK and SNARK EDITOR codes both need about 50 blocks of 512 words of store on Atlas. Of this, only about nine blocks are actually used for data by the EDITOR, six blocks by SNARK, the remainder being program and library routines. Most of the computing time was required by SNARK which took approximately 6 sec to integrate each of the 33 S_{ij} arrays through about 70–75 steps. The running time decreased to about 4 sec for each S_{ij} array when symmetry was used to reduce the number of differential equations needing solution. Another minute was required for tabulating the atmospheric parameters and calculating the integration coefficients. The EDITOR run was completed in about one minute.

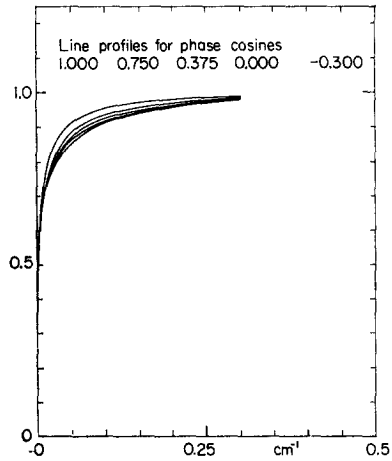

FIG. 8. Computed absorption line profiles for the $J = 18$ line for various values of $\bar{\mu}$. The curves can be discriminated by observing that the absorption is an increasing function of $\bar{\mu}$.

APPENDIX A. DERIVATION OF EQ. (2.2)

We give an elementary vector derivation. Choose a master set of axes (**I**, **J**, **K**), an orthonormal triad with K directed from the center of Venus towards the earth. Define the phase angle α by $\alpha = \cos^{-1}\bar{\mu}$, so that if the plane containing Sun, Earth, and Venus is perpendicular to J, the Sun is in the direction

$$\mathbf{L} = \sin\alpha\,\mathbf{I} + \cos\alpha\,\mathbf{K}\,. \tag{1}$$

Likewise, in the master axes, a point on the surface of Venus has coordinates $(\sin\Theta\cos\Phi,\ \sin\Theta,\ \sin\Phi\cos\Theta)$. At this point we construct a local system of axes with an orthonormal triad $(\mathbf{i}, \mathbf{j}, \mathbf{k})$, where $\mathbf{i}$ is in the direction of increasing Θ, $\mathbf{j}$ in the direction of increasing Φ, and $\mathbf{k}$ in the local vertical so that

$$\begin{aligned}\mathbf{i} &= (\cos\Theta\cos\Phi,\ \cos\Theta\sin\Phi,\ -\sin\Theta),\\ \mathbf{j} &= (-\sin\Phi,\ \cos\Phi,\ 0),\\ \mathbf{k} &= (\sin\Theta\cos\Phi,\ \sin\Theta\sin\Phi,\ \cos\Theta)\end{aligned} \tag{2}$$

in the master axes. In the local axes a vector in the direction having polar coordinates $\theta(=\cos^{-1}\mu)$ and φ has Cartesian coordinates $(\sin\theta\ \cos\varphi,\ \sin\theta\ \sin\varphi,\ \cos\theta)$. The reflected beam is in the direction $\mathbf{K}$, which defines

$$\theta = \Theta, \quad \varphi = \pi \tag{3}$$

at the point (Θ, Φ) on the planetary surface. Similarly, the incident beam is in the direction $-\mathbf{L}$ so that

$$\begin{aligned}1 \geq \mu_0 &= \mu\bar{\mu} + [(1-\mu^2)(1-\bar{\mu}^2)]^{1/2}\cos\Phi \geq 0,\\ \tan\varphi_0 &= -\frac{(1-\bar{\mu}^2)^{1/2}\sin\Phi}{\mu(1-\bar{\mu}^2)^{1/2}\cos\Phi - \bar{\mu}(1-\mu^2)^{1/2}}.\end{aligned} \tag{4}$$

We can now calculate the specific intensity in the direction of the earth by averaging over that part of the planet's surface defined by (4), so that

$$I_\nu(\bar{\mu}) = \int I_\nu(\mu, \varphi)\, d\Sigma/\pi a^2, \tag{5}$$

where a is the radius of the radiating surface, and $d\Sigma$ is the projected element of area on a plane normal to $\mathbf{K}$. Thus

$$\begin{aligned}d\Sigma/\pi a^2 &= a^2\sin\Theta\, d(-\sin\Theta)\, d\Phi/\pi a^2\\ &= \mu\, d\mu\, d\Phi/\pi\end{aligned}$$

by (3), and so by (5) and (2.1)

$$I_\nu(\bar{\mu}) = \frac{F_\nu}{4\pi}\int_0^1 d\mu \int d\Phi\, S_\nu(\mu, \pi; \mu_0, \varphi_0). \tag{6}$$

Changing to integration variables μ, μ_0 instead of μ, Φ and allowing for symmetry, we obtain (2.2).

Appendix B. Truncation Error in Spline Interpolation

For simplicity we consider only uniformly spaced joints $\mu_k = kl$, $0 \leq k \leq N$, $1 = N^{-1}$. We can then use finite-difference operators and write (3.8) in the form

$$g_{k+1/2} = \delta^2 f_k - g_{k-1/2}, \quad 1 \leq k \leq N-1 \tag{1}$$

and (3.9) in the form

$$\begin{aligned} g_{1/2} &= [1 - (1 + lD)E^{-1}]f_1 \\ &= (\tfrac{1}{2} l^2D^2 - \tfrac{1}{3} l^3D^3 + \ldots)f_1. \end{aligned} \tag{2}$$

It is then easy to establish by repeated application of (1) together with $E^{-1} = e^{-lD}$ (Taylor series operator) that

$$\begin{aligned} g_{2n+1/2} &= (\tfrac{1}{2} l^2D^2 + \tfrac{1}{6} l^3D^3 + \ldots)f_{2n} \qquad n = 1, 2, \ldots \\ g_{2n+3/2} &= (\tfrac{1}{2} l^2D^2 + \tfrac{1}{3} l^3D^3 + \ldots)f_{2n+1} \qquad n = 0, 1, 2, \ldots \end{aligned} \tag{3}$$

Now for $\mu = (k + \theta)l$, $0 \leq \theta \leq 1$, we have the Taylor series expansions

$$\begin{aligned} f(\mu) &= \exp(\theta lD) f_k = \exp[-(1-\theta)lD] f_{k+1} \\ &= (1-\theta)\exp(\theta lD) f_k + \theta \exp[-(1-\theta)lD] f_{k+1} \\ &= (1-\theta) f_k + \theta f_{k+1} + \{\exp[\theta lD] - 1 + \theta(1 - \exp[lD])\} f_k \\ &= (1-\theta) f_k + \theta f_{k+1} - \theta(1-\theta)[\tfrac{1}{2} l^2D^2 + \tfrac{1}{6}(1+\theta) l^3D^3 + \ldots] f_k . \end{aligned} \tag{4}$$

Comparison with (3.6), which can be put in the form

$$\Phi_{k+1/2}(f; \mu) = (1-\theta) f_k + \theta f_{k+1} - g_{k+1/2}\theta(1-\theta),$$

immediately gives the truncation error

$$\begin{aligned} R_{k+1/2}(f; \mu) &= f(\mu) - \Phi_{k+1/2}(f; \mu) \\ &= \begin{cases} -\tfrac{1}{6}\theta^2(1-\theta) l^3 f_k''' + \ldots & \text{for } k = 0, 2, 4, \ldots \\ +\tfrac{1}{6}\theta(1-\theta)^2 l^3 f_k''' + \ldots & \text{for } k = 1, 3, 5, \ldots, \end{cases} \end{aligned} \tag{5}$$

where we write f_0''' for f_1''' in the case $k = 0$. [As Eq. (3.4) shows, derivatives of $f(\mu)$ higher than the first do not exist at $\mu = 0$, and we make this definition of f_0''' for the sole purpose of preserving symmetry in Eq. (5)].

The corresponding error in $\varphi(\tau; \mu)$ can be written

$$R^*(\varphi; \mu_i) = \frac{1}{2} \int_0^1 \frac{R(f; \mu')\, d\mu'}{\mu'}$$

$$= \frac{1}{12} \sum_{k=0}^{N-1} l^3(-1)^{k+1} f_k''' \int_0^1 \frac{\Psi_k(\theta)}{k+\theta}\, d\theta$$

where

$$\Psi_k(\theta) = \theta^2(1-\theta) \quad \text{for } k \text{ even}$$

$$= \theta(1-\theta)^2 \quad \text{for } k \text{ odd}.$$

For $k = 0$,

$$\int_0^1 \frac{\Psi_k(\theta)}{\theta}\, d\theta = \frac{1}{6},$$

and clearly

$$\int_0^1 \frac{\Psi_k(\theta)}{k+\theta}\, d\theta < \int_0^1 \frac{\Psi_k(\theta)}{\theta}\, d\theta = \begin{cases} \frac{1}{6} \text{ if } k \text{ is even} \\ \frac{1}{3} \text{ if } k \text{ is odd} \end{cases}$$

Thus

$$| R^*(\varphi; \mu_i) | < \frac{1}{12} l^3 M \left(\frac{N}{4}\right) = \frac{Ml^2}{48}$$

when N is even, giving the formula quoted in the text.

REFERENCES

1. J. W. CHAMBERLAIN, *Astrophys J.* **141**, 1184 (1965).
2. J. W. CHAMBERLAIN and G. P. KUIPER, *Astrophys. J.* **124**, 399 (1956).
3. H. SPINRAD, *Proc. Astron. Soc. Pacific.* **74**, 187 (1962).
4. S. CHANDRASEKHAR, "Radiative Transfer," Chap. 7. Dover, New York (1960).
5. I. W. BUSBRIDGE, *Astrophys J.* **133**, 198 (1961).
6. R. E. BELLMAN, R. E. KALABA, and M. C. PRESTRUD, Invariant imbedding and radiative transfer in slabs of finite thickness, *in* "Modern Analytic and Computational Methods in Science and Mathematics," Vol. 1 (R. E. Bellman and R. E. Kalaba, Eds.). Elsevier, New York (1963).
7. R. H. MERSON, Proceedings of a Symposium on Data Processing, Weapons Research Establishment, Salisbury, South Australia (1957).
8. D. F. Mayers, *in* "Integration of Ordinary and Partial Differential Equations" (L. Fox, Ed.), Chap. 2. Pergamon, Oxford, England (1962).
9. L. D. KAPLAN, A Preliminary Model of the Venus Atmosphere, Jet Propulsion Laboratory Technical Report No. 32–379, 1962.